

## Solitonic lattices in photorefractive crystals

M. Petrović,<sup>1</sup> D. Träger,<sup>2</sup> A. Strinić,<sup>1</sup> M. Belić,<sup>1</sup> J. Schröder,<sup>2</sup> and C. Denz<sup>2</sup>

<sup>1</sup>*Institute of Physics, P.O. Box 57, 11001 Belgrade, Serbia*

<sup>2</sup>*Institute of Applied Physics, Westfälische Wilhelms-Universität Münster, D-48149 Münster, Germany*

(Received 20 June 2003; published 24 November 2003)

Two-dimensional spatial solitonic lattices are generated and investigated experimentally and numerically in a  $\text{Sr}_x\text{Ba}_{1-x}\text{Nb}_2\text{O}_6:\text{Ce}$  crystal. An enhanced stability of these lattices is achieved by exploiting the anisotropy of coherent soliton interaction, in particular the relative phase between soliton rows. The manipulation of individual soliton channels is achieved by the use of supplementary control beams.

DOI: 10.1103/PhysRevE.68.055601

PACS number(s): 42.65.Tg, 42.65.Sf, 05.45.Yv

Wide ( $\sim 1$  mm) Gaussian beams launched in a photorefractive (PR) crystal in the self-focusing regime tend to break into spatially disordered arrays of filaments, owing to transverse modulational instabilities [1]. However, ordered arrays of Gaussian beamlets ( $\sim 10$   $\mu\text{m}$ ), launched in conditions appropriate to the generation of spatial screening solitons [2], form much more stable solitonic lattices. Weakly interacting pixel-like arrangements of solitons that can individually be addressed are interesting for applications as self-adaptive waveguides [3,4].

Adaptive waveguides are of particular interest in all-optical information processing for their potential to generate large arrays, as well as for allowing many configurations with different interconnection possibilities. Spatial optical solitons are natural candidates for such applications, owing to their ability for self-adjustable waveguiding and versatile interaction capabilities, as demonstrated in light-induced  $Y$  and  $X$  couplers, beam splitters, directional couplers, and waveguides. In addition to such few-beam configurations, the geometries with many solitons propagating in parallel—the so-called soliton pixels, arrays, or lattices—have been suggested for applications in information processing and image reconstruction [5–8]. Recently several groups demonstrated the formation of quadratic arrays of solitons in parametric amplifiers [8,9] and PR media, with coherent [7,10] and incoherent [4] beams.

In this Rapid Communication we combine the properties of spatial PR solitons to form pixel-like lattices, to investigate experimentally and numerically the generation and interactions in large arrays of spatial solitons. We achieve improved stability of solitonic lattices by utilizing an anisotropic interaction between solitons, in particular the phase-dependent interaction between solitonic rows. We manipulate individual or pairs of solitons using incoherent and phase-sensitive control beams.

The creation of solitonic lattices requires the stable non-interacting propagation of arrays of self-focusing beams. A crucial feature in the parallel propagation of PR spatial solitons is their anisotropic mutual interaction [11]. Because the refractive index modulation induced by a single soliton reaches beyond its effective waveguide, phase-dependent coherent as well as separation-dependent incoherent interactions, such as repulsion or attraction, may appear between the neighboring array elements. These interactions also affect the waveguiding characteristics of an individual solitonic

channel. Therefore, the separation between solitons and their nearest-neighbor (NN) arrangement, determined by the form of the lattice, must carefully be chosen so as to minimize all forms of interaction. In our experiments, as well as numerical simulations, we determine the critical soliton distances for the given crystal thickness at which the interaction becomes noticeable. To achieve closer packing of solitons, while maintaining propagation without interaction, the phase relationship between different beams in the array is exploited.

The creation of lattices and controlling individual pixels is explored in the experimental setup of Fig. 1. A laser beam derived from a frequency-doubled Nd:YAG (yttrium aluminum garnet) laser emitting at 532 nm illuminates a spatial light modulator (SLM), which imprints the image of a spot-array onto the beam. The spatial light modulator in turn is imaged onto the front face of a photorefractive  $\text{Sr}_{0.60}\text{Ba}_{0.40}\text{Nb}_2\text{O}_6:\text{Ce}$  (SBN60:Ce) crystal ( $5 \times 5 \times 20$  mm), which is positioned so that the propagation direction is along the 20 mm axis. To exploit the dominant electro-optic component  $r_{33} \approx 200$  pm/V of our SBN sample, the incident laser beam is linearly polarized parallel to the  $c$  axis of the crystal, perpendicular to the propagation direction. Regular patterns of up to  $25 \times 25$  spots, each with the diameter of about  $20$   $\mu\text{m}$  and an intensity of 110 nW, are imaged onto the front face of the crystal. Applying an external dc electric field of about 1 kV/cm across the crystal and illuminating the crystal with a uniform white light to induce an artificial dark conductivity creates appropriate conditions for the formation of spatial screening solitons. To manipulate individual or pairs

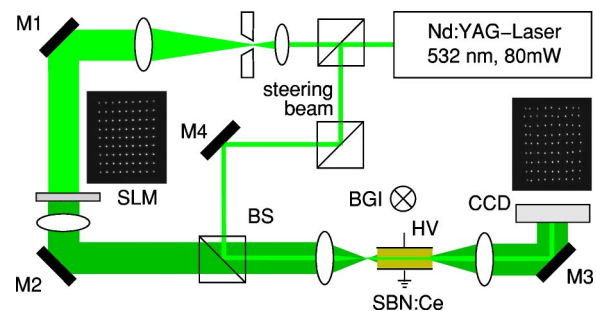


FIG. 1. Experimental setup for the creation of solitonic lattices and the control of individual pixels. Insets: typical input and output arrays.

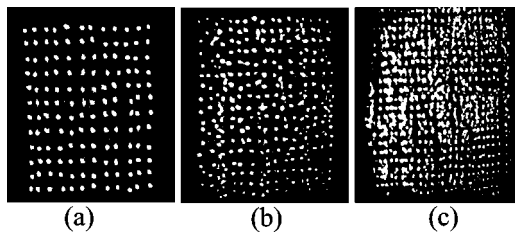


FIG. 2. Experimental rectangular solitonic lattices after 20 mm propagation. (a) Above-critical  $12 \times 12$  array with  $\Delta x = 70 \mu\text{m}$ ,  $\Delta y = 85 \mu\text{m}$ . (b) Slightly below-critical  $17 \times 17$  array with  $\Delta x = 60 \mu\text{m}$ ,  $\Delta y = 75 \mu\text{m}$ . (c) Below-critical  $25 \times 25$  array with  $\Delta x = 50 \mu\text{m}$ ,  $\Delta y = 65 \mu\text{m}$ .

of solitons in the lattice, an additional control beam is derived from the same laser. It is our experience that large arrays of solitons can easily be formed in PR crystals. The larger the array the less significant the finite size (edge) effects. The number of pixels is mainly limited by the aperture of the PR crystal and the resolution of the inducing SLM. One can tailor the arrangement of beams according to specific needs.

Propagation without mutual interaction requires sufficient initial distance between beams. It also depends on other parameters influencing the soliton formation and propagation, such as the initial beam profiles and phases, and the strength of the nonlinearity, but less crucially. A distance smaller than the critical distance for coherent interaction between solitons leads to their attraction and eventual fusion. The attractive interaction is more pronounced along the  $y$ -transverse direction, perpendicular to the direction of the external field. For a given propagation distance this is reflected in the deformed appearance of the lattice. Deformations may also be caused by the crystal inhomogeneities that cannot be controlled. Hence the determination of the critical distance is qualitative, based on the inspection of a series of runs with decreasing intersoliton distances. A typical series of runs is depicted in Fig. 2, where the distance between solitons is reduced by increasing the density of packing. An estimate of the critical distance is found to lie between 3 and 4 beam diameters for in-phase arrays in our experimental conditions. It is slightly larger in the  $y$  direction than in the  $x$  direction. This estimate is corroborated in numerical simulations.

Our numerical simulations are based on the paraxial approximation to the anisotropic propagation of coherent optical beams in saturable PR media,

$$2ikn_0\partial_z A + \nabla_{\perp}^2 A = -k^2 n_0^4 r_{33}(\partial_x \phi)A, \quad (1)$$

where  $k$  is the wave number in vacuum,  $n_0 \approx 2.35$  is the bulk refractive index,  $\nabla_{\perp}^2$  is the transverse Laplacian, and  $A$  the slowly varying envelope of the electric field of the beam. The paraxial equation is augmented with the equation for the electrostatic potential  $-\nabla \phi = \mathbf{E}$  of the space-charge field  $\mathbf{E}$  generated in the crystal [12,13]

$$\nabla^2 \phi + \nabla \phi \cdot \nabla \ln(1+I) = E_e \partial_x \ln(1+I), \quad (2)$$

where  $E_e$  is the external field. The light intensity  $I$  is normalized to the background intensity. These equations are solved

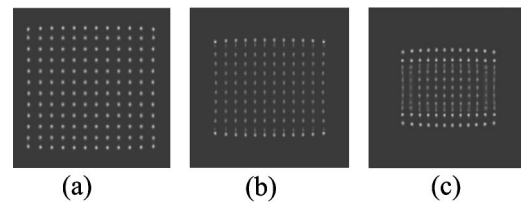


FIG. 3. Quadratic  $12 \times 12$  in-phase solitonic lattice after 35 mm propagation, numerical. Electro-optic coefficient  $210 \text{ pm/V}$ , external electric field  $900 \text{ V/cm}$ . The total size of data windows is  $1 \text{ mm}^2$  and the initial full width at half maximum (FWHM) size of individual beams  $20 \mu\text{m}$ . (a)  $\Delta x = \Delta y = 70 \mu\text{m}$ . (b)  $\Delta x = \Delta y = 60 \mu\text{m}$ . (c)  $\Delta x = \Delta y = 50 \mu\text{m}$ .

together, in the manner described in Ref. [14]. Behavior qualitatively similar to the experimental was found: Parallel propagation of coherent solitons with varying separation can be adjusted to be almost without interaction [Fig. 3(a)] whereas for separations below the critical length the fusion of soliton columns is observed [Figs. 3(b) and 3(c)].

The propagation of incoherent lattices was found to be more stable than the propagation of coherent in-phase lat-

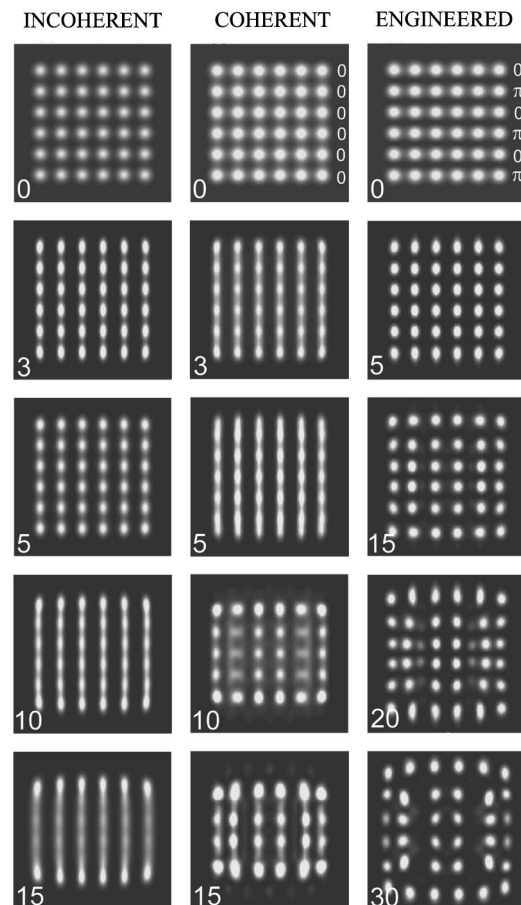


FIG. 4. Comparing the propagation of  $6 \times 6$  subcritical square arrays with  $40 \mu\text{m}$  NN separation, for different propagation distances, given in mm in each figure. Left column an incoherent lattice, middle column a coherent in-phase lattice, and right column a phase-engineered lattice. Numbers 0 and  $\pi$  in the two upper right figures indicate the phase difference between the adjacent rows of solitons. Other parameters as in Fig. 3.

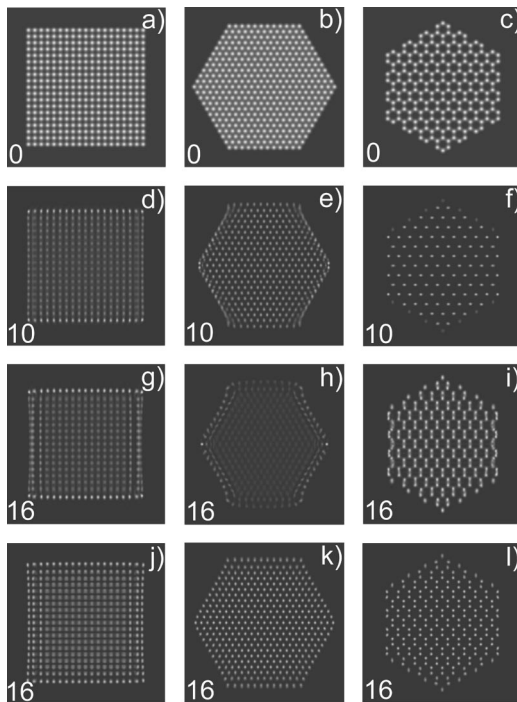


FIG. 5. Propagation of square, hexagonal, and honeycomb solitonic lattices with  $40 \mu\text{m}$  NN separation. (a)–(c) Initial intensity distributions. (d)–(f) In-phase lattices propagated for 10 mm. Note in (f) the inversion of the honeycomb lattice. (g)–(i) In-phase lattices propagated for 16 mm. Strong edge deformation is evident. (j)–(l) The same lattices, but with alternate rows of solitons out of phase, propagated for 16 mm. Other parameters as in Fig. 3.

tices for identical conditions; however, our intention is to exploit the possibility of manipulating the distribution of phase across the lattice, to achieve closer packing while maintaining propagation without interaction. The comparison among incoherent, coherent, and phase-engineered lattices is provided in Fig. 4. The NN separation is  $40 \mu\text{m}$ , which is about half the critical distance from Fig. 2 and twice the FWHM of initial beams. It was found that the best results are obtained when the adjacent rows of solitons are out of phase. This is in agreement with theoretical expectations of the anisotropic interaction: Along rows the solitons are in phase, and along columns they are out of phase, which makes the interaction between them universally repulsive and leads to enhanced stability. It is seen that the phase-engineered lattice in the right column of Fig. 4 is much more stable than the incoherent or coherent in-phase lattices in the left and central columns (note also different propagation distances). For smaller lattices, as in Fig. 4, the edge effects are also more pronounced.

To further test the idea of phase engineering for enhancing the stability, different lattices were formed and propagated (Fig. 5). It is seen that the in-phase lattices deform fast, and that after 10 mm of propagation, owing to the attractive forces along the  $y$  direction, some rows are lost in the quadratic lattice, while the hexagonal and honeycomb lattices are strongly deformed. The honeycomb lattice deforms continually from the direct to the inverse (hexagonal) lattice and back [Figs. 5(f) and 5(i)]. However, out-of-phase lattices for

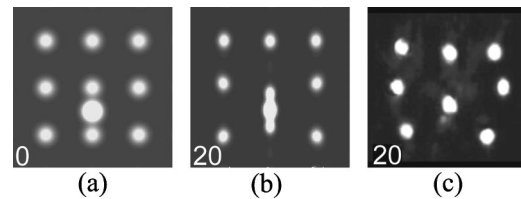


FIG. 6. Comparing numerical and experimental action of a control beam, placed midway between two pixels. (a) Initial configuration. (b) Numerical situation after 20 mm propagation. (c) The corresponding experimental situation. The data are  $70 \mu\text{m}$  pixel separation, each spot  $20 \mu\text{m}$  in diameter, coherent lattice, incoherent control. The control beam is three times more intense than any of the pixels.

identical initial conditions and at a longer propagation distance of 16 mm are only slightly deformed. It is also evident that the edge effects decrease with increasing the lattice size.

Use of solitonic arrays for applications in information technology requires means of manipulating individual waveguides, so as to combine different channels, separate them, or induce energy exchange between the channels. For this purpose the well-known interaction effects of spatial PR solitons can be exploited [2,7]. We utilize here a supplementary steering control beam derived from the Nd:YAG laser that can be focused anywhere on the front face of the crystal. Varying the phase of the control beam relative to the phase of array elements, a phase-sensitive coherent or incoherent interaction can be induced that may lead to fusion or repulsion of different solitons in the array. Early experimental results

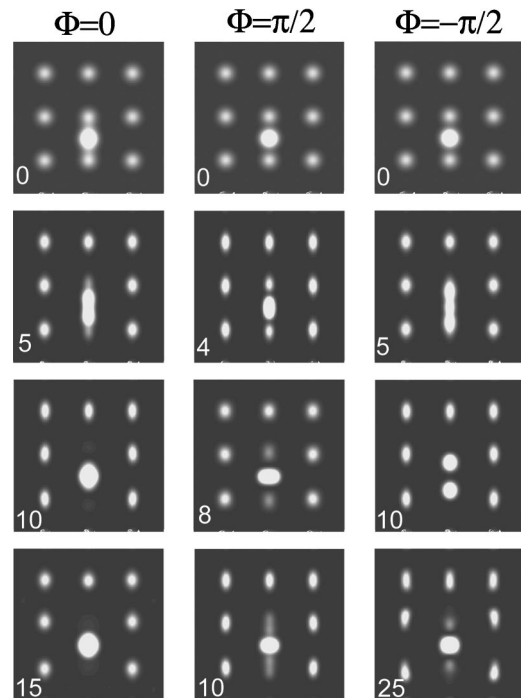


FIG. 7. Illustrating the action of a phase-sensitive control beam in a coherent square lattice with  $70 \mu\text{m}$  NN separation. Phase shift of the control beam relative to the lattice solitons is indicated on the top of each column. Numbers within each figure indicate the propagation distance in mm. Other parameters are as in Fig. 3.

on an incoherent control were presented in Refs. [3,4,7,10]. Here we display the comparison with experiment, using an incoherent control beam acting on a pair of coherent pixels (Fig. 6). The data are as in the experiment of Refs. [7,10]. Qualitative agreement is visible.

The action of a phase-sensitive control beam is depicted in Fig. 7. We chose to present the cases of 0 and  $\pm\pi/2$  phase shifts of the control beam relative to the lattice. While for the zero phase shift the merging of the two channels is seen, in the case of  $\pm\pi/2$  a strong energy exchange between the control beam and the solitons is observed. For the  $\pi/2$  phase shift the energy flows from the pixels to the control beam, so that at approximately 9 mm the control beam is maximally bright and the pixels are extinguished. For the phase shift of  $-\pi/2$  the flow of energy is from the control beam to the pixels. At approximately 10 mm the control beam is extinguished, and the two slightly displaced pixels are maximally bright. For the zero phase shift the three beams gradually merge, so that at approximately 15 mm only one beam is visible. Afterwards the cycles for the three values of the phase shift repeat in the inverse order, but less clearly visible, and some energy is transferred to the adjacent pixels (not shown).

In summary, we have investigated several aspects of the interaction of solitons arranged in lattices for possible use in all-optical waveguides and interconnects. We have displayed experimentally the formation of large two-dimensional arrays of solitons that can be used to guide light at different wavelengths. Increased stability of solitonic lattices is achieved by the phase engineering of soliton rows. We have shown how to use a supplementary steering beam to fuse, extinguish, or enhance selected channels in the solitonic lattice. Our numerical simulations, based on the anisotropic model of PR solitons, are in qualitative agreement with experimental results.

A.S. and M.B. gratefully acknowledge financial support from the Alexander von Humboldt Foundation, for the stay and work at WWU Münster. D.T. acknowledges support from the Konrad-Adenauer-Stiftung. Parts of this work were supported by the Graduiertenkolleg “Nichtlineare kontinuierliche Systeme” of the Deutsche Forschungsgemeinschaft. Work at the Institute of Physics is supported by the Ministry of Science, Technologies, and Development of the Republic of Serbia, under grants OI 1475 and 1478. We thank Dr. Jürgen Petter, Institut für Angewandte Physik, TU Darmstadt, for help in the experiment on pixel control.

- 
- [1] A.V. Mamaev, M. Saffman, D.Z. Anderson, and A.A. Zozulya, *Phys. Rev. A* **54**, 870 (1996).
  - [2] For an overview see the special issue on solitons, edited by M. Segev, *Opt. Photonics News* **13**, 2 (2002).
  - [3] J. Petter and C. Denz, *J. Opt. Soc. Am. B* **19**, 1145 (2002).
  - [4] Z. Chen and K. McCarthy, *Opt. Lett.* **27**, 2019 (2002).
  - [5] P.V. Mamyshev, C. Bosshard, and G.I. Stegeman, *J. Opt. Soc. Am. B* **11**, 1254 (1994).
  - [6] W. Krolikowski and Yu.S. Kivshar, *J. Opt. Soc. Am. B* **13**, 876 (1996).
  - [7] C. Weilmann, M. Ahles, J. Petter, D. Träger, J. Schröder, and C. Denz, *Ann. Phys. (Leipzig)* **9**, 1 (2002).
  - [8] A. Bramati, W. Chinaglia, S. Minardi, and P. Di Trapani, *Opt. Lett.* **26**, 1409 (2001).
  - [9] S. Minardi, S. Sapone, W. Chinaglia, P. Di Trapani, and A. Berzanskis, *Opt. Lett.* **25**, 326 (2000).
  - [10] J. Petter, J. Schröder, D. Träger, and C. Denz, *Opt. Lett.* **28**, 438 (2003).
  - [11] W. Krolikowski, M. Saffman, B. Luther-Davies, and C. Denz, *Phys. Rev. Lett.* **80**, 3240 (1998).
  - [12] A.A. Zozulya and D.Z. Anderson, *Phys. Rev. A* **51**, 1520 (1995).
  - [13] M.R. Belić, D. Vujić, A. Stepken, F. Kaiser, G.F. Calvo, F. Agullo-Lopez, and M. Carrascosa, *Phys. Rev. E* **65**, 066610 (2002).
  - [14] A. Stepken, F. Kaiser, and M.R. Belić, *J. Opt. Soc. Am. B* **17**, 68 (2000).